Non-diffusive transport and anisotropic thermal conductivity in high-density Pt/Co superlattices

Mohammadreza Shahzadeh[1], Olga Andriyevska[2], Ruslan Salikhov[3], Lorenzo Fallarino[3], Olav Hellwig[3,4], Simone Pisana[1,2,]*

1. Department of Electrical Engineering and Computer Science, York University, 4700 Keele Street, Toronto ON, M3J 1P3, Canada

2. Department of Physics and Astronomy, York University, 4700 Keele Street, Toronto ON, M3J 1P3, Canada

3. Institute of Ion Beam Physics and Materials Research, Helmholtz-Zentrum Dresden-Rossendorf, Bautzner Landstraße 400, 01328 Dresden, Germany

4. Institute of Physics, Technische Universität Chemnitz, Reichenhainer Straße 70, 09126 Chemnitz, Germany

* Corresponding Author: simone.pisana@lassonde.yorku.ca

ABSTRACT

Despite the numerous reports over the last two decades dedicated to the study of interfacial thermal transport, physics of thermal transport across nanoscale metallic multilayers is less explored. This is in part due to the relatively high conductance characteristic of these interfaces, which renders them difficult to characterize. Interfacial transport in these systems has so far appeared to be diffusive – a surprising behavior when the interface density increases and the layer thicknesses become comparable with mean free path of electrons. To address the limit of diffusive theories describing heat transport across high-density metallic interfaces, we systematically investigate heat transport in and across Pt/Co multilayers via frequency domain thermoreflectance. Sensitivity gained from offsetting the laser beam and reducing laser spot size allows for the measurement of anisotropic thermal conductivity of the multilayers. By changing the number of interfaces while keeping the overall thickness of Pt and Co in the multilayer structure constant, the effect of interface density on the multilayers' effective thermal conductivity is studied. The extracted Pt/Co interface thermal boundary conductance is then compared to the calculations from the electronic diffuse mismatch model and experimental data available in literature. We show that as the multilayer period thickness becomes much smaller than the electron mean free path, measurements markedly deviate from the diffusive transport theory. We attribute this deviation to the non-diffusive nature of heat transport in sub-nanometric scales at interface densities above 1/nm.

KEYWORDS

Heat transport, metallic multilayers, anisotropic thermal conductivity, non-diffusive transport, frequency-domain thermoreflectance.

1. Introduction

Metallic multilayers have attracted a substantial amount of attention due to their impact in fields such as magnetic memory [1,2] and spintronics [2-5] as well as due to their high mechanical strength at the nanometric scale [6-8]. Thanks to high electrical conductivity at metallic interfaces, thermal transport in metallic multilayers is often more efficient compared to metal/dielectric multilayers in which phonon-mediated transport dominates. Despite this, thermal resistance across metallic multilayers can still be an important barrier against heat transfer, particularly when a high interface density between the heat source and the heat sink limits heat dissipation. This heat transport hindrance can, for instance, be a desirable attribute in thermal management applications [9] or compromise the thermal stability of spintronic devices [2] and heat-assisted magnetic recording components [10]. So far, little work has been done on heat transport in nanometric and sub-nanometer metallic multilayers, where the electron mean free path ℓ approaches or exceeds the individual layer thickness and heat transport deviates from the diffusive Fourier regime, posing fundamental questions that can be of importance in the application of metallic multilayers.

Heat transport is anisotropic in multilayers, and heat is carried in-plane more readily compared to out-of-plane [9, 11-14]. This is mainly due to the increased resistance in the out-of-plane direction originating from the presence of the interfaces. Although recent advances in optical metrology techniques have enabled researchers to study heat transport across different interfaces [15,16], most of the studies so far have focused on metal/non-metal or non-metal/non-metal structures. Gundrum *et al*. measured the room temperature thermal boundary conductance (G) of the Al/Cu interface to be 4 GW/m^{2}K, which is an order of magnitude larger than interfaces with phonon-mediated transport [17]. Wilson and Cahill measured the effective thermal conductivity

of Pd/Ir multilayers and found G to be 14 ± 3 GW/m^{2}K. This is the highest value reported so far [18]. Cheaito *et al*. compared results presented for Al/Cu [17] and Pd/Ir [18] interfaces to Cu/Nb interfaces, demonstrating that the temperature derivative of the electron energy flux predominantly affects G, whereas the transmission probability given by the interfacial mismatch in electronic properties is less important [19]. This is unlike phonon-mediated interfaces in which G is more dependent on interfacial phonon mismatch.

Measuring G in metallic and highly conductive interfaces requires high measurement sensitivity due to the low contribution it has on the overall thermal resistance of the system. Therefore, studies have generally either concentrated on samples having hundreds of interfaces or have been able to provide only a lower bound value for G. In this regard, lower bounds of 8 GW/m^{2}K and 5 GW/m^{2}K have been reported for G in Pt/Co [20] and Pt/Au [21] interfaces, respectively.

To quantify electron-mediated heat transport at metallic interfaces, an electronic extension to the commonly used diffuse mismatch model (DMM) used to describe phonon-mediated transport has been successfully employed [17-19,22]. The electronic DMM (EDMM), introduced by Gundrum *et al*. [17], considers diffuse interface scattering and temperature-independent density of states for a degenerate metal with an isotropic Fermi surface. The resulting relation to describe G is a function of the electronic heat capacity and Fermi velocities of the metals adjacent the interface, and it does not depend on layer thickness.

To the best of our knowledge, there is no evidence in the literature that G in metallic multilayers is affected by non-diffusive transport or deviates from the EDMM theory. Previous work has highlighted that diffuse scattering at metal interfaces seems to be an assumption that is consistent with experimental observations [17,18], and that for layer thickness as low as ~ℓ/3

transport is consistent with Fourier's law [18,23]. In other words, if transport at metal interfaces can be treated as diffusive even when the constituent layer thickness is small, then the effective thermal resistance across the structure will simply be given by the sum of the layer thermal resistance and the interface resistance. This appears to be in contradiction with other instances where diffusive thermal transport breaks down. For example, the apparent thermal conductivity of a thin semiconductor slab is reduced with respect to its bulk value when the slab thickness becomes comparable to the phonon mean free path [24].

In metal multilayers, two reasons why transport would be characterized as diffusive even when interfaces are closer than ℓ are that (1) the interfaces may induce mostly elastic scattering, or that (2) interface scattering does not alter the electronic energy for its distribution to deviate significantly from equilibrium. This raises several questions. When does the assumption of diffusive interface scattering break down so that G is no longer constant as the interface density increases? Would one observe a minimum in the effective thermal conductivity in metallic multilayers? [25] These are the very questions that we are addressing here. The anisotropic thermal conductivity of Pt/Co multilayers is measured at room temperature with interface densities approaching 2/nm (about one order of magnitude below ℓ of 7-10 nm for Pt [20] and 5-12 nm for Co [23,26]). The value for G of Pt/Co is then extracted and compared with expectations from EDMM [17]. We show that as the interface density increases, a deviation from the model is observed. We attribute this deviation to non-diffusive transport at sub-nanometric scales.

2. Experimental Methods

The samples studied in this work are layered as Pt(2)/[Pt(t_{Pt})/Co(t_{Co})]$_q$/Pt(20)/Ta(1.5)/SiO_2(100)/Si, where the numbers in parenthesis t_{Pt} and t_{Co}

are the Pt and Co layer thickness in nm (Table 1), and q is the number of Pt/Co repeats. The topmost 2 nm Pt layer is introduced to prevent oxidation of the Co layer beneath. Note that we have prepared two samples at the highest interface density having different total thickness by varying the total number of Pt/Co repeats. Otherwise, the total thickness of Co and Pt is kept constant. The multilayers were deposited at room temperature using an AJA magnetron sputtering system at a base pressure of 1.7×10^{-7} Torr and sputtering Ar pressure of 3 mTorr. The thickness of all layers is measured by X-Ray reflectivity. Additionally, high-resolution cross-sectional transmission electron microscopy confirms that the structure is smooth, and each layer in the structure remains continuous with a well-defined interface to neighboring layers, down to the thinnest layers studied here of 0.4 nm for Co and 0.7 nm for Pt [27,28].

Table 1. Characteristics of the multilayers studied in this work. t_{ML} represents the total thickness of the Pt(2)/[Pt(t_{Pt})/Co(t_{Co})]$_q$/Pt(20)/Ta(1.5) layers, k_r is the in-plane thermal conductivity measured by 4-point probe, and C_{ML} is the volumetric heat capacity of these layers calculated using a weighted average of the volumetric heat capacities of Pt and Co.

	Sample Structure	t_{ML}(nm)	k_r (W/mK)	C_{ML} (MJ/m^{3}K)
ML-1	[Pt(0.7nm)/Co(0.4nm)]$_{128}$	164.3	15.0	3.34
ML-2	[Pt(0.7nm)/Co(0.4nm)]$_{64}$	93.9	17.2	3.28
ML-3	[Pt(2.8nm)/Co(1.6nm)]$_{32}$	164.3	22.2	3.34
ML-4	[Pt(11.2nm)/Co(6.4nm)]$_8$	164.3	33.0	3.34
ML-5	[Pt(44.8nm)/Co(25.6nm)]$_2$	164.3	39.8	3.34

The anisotropic thermal properties of the multilayers are measured by frequency domain thermoreflectance (FDTR) [29]. A beam-offset approach was utilized to increase the sensitivity to the in-plane component of the thermal conductivity [30]. The FDTR setup schematic is shown

in Figure 1(a) [29,30]. A continuous-wave laser (Omicron A350 operating at 515 nm) is intensity-modulated using a lock-in amplifier (Zurich Instruments HF2LI) over a range of frequencies up to ~20 MHz. This pump laser is absorbed on the sample surface, introducing heat flux at the desired modulation frequency. Another continuous-wave laser (Omicron A350 operating at 785 nm) then probes the resulting sample surface temperature fluctuations through changes in temperature-dependent reflectivity. The reflected light is then collected using a photodetector (Thorlabs PDA8A) and demodulated using the lock-in amplifier. By introducing a laser beam offset between pump and probe (1.25 μm at the sample surface) and small laser spot size (typically 1.4 μm $1/e^2$ diameter), the signal magnitude and the sensitivity to in-plane thermal transport is improved.

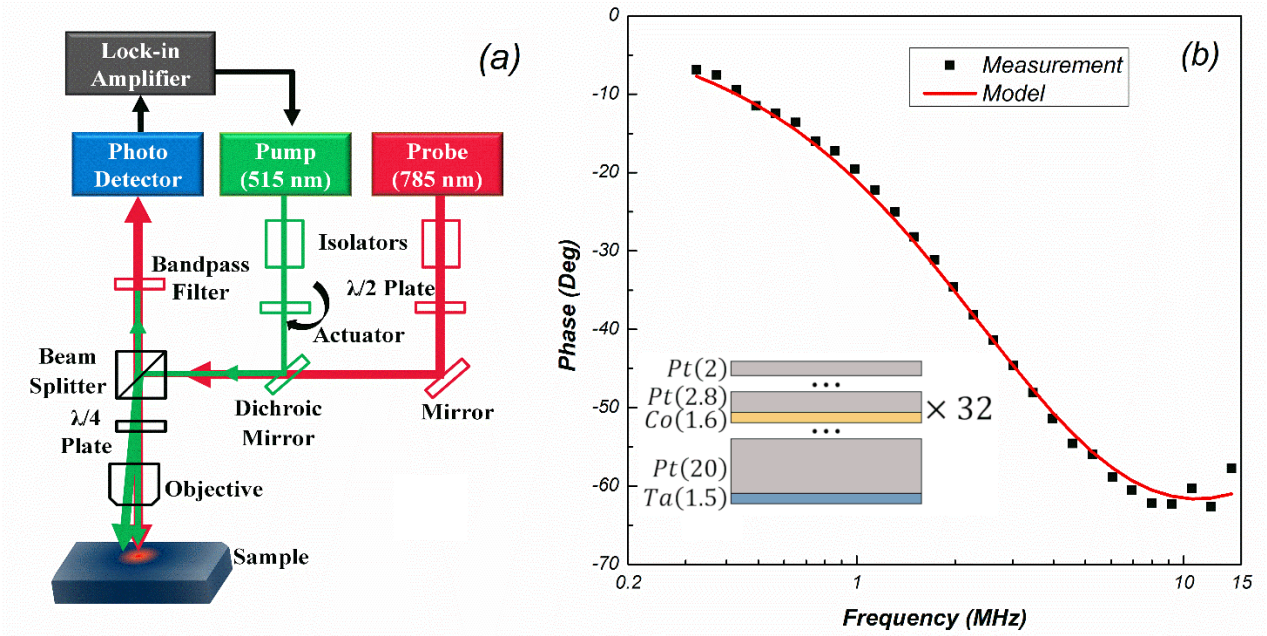

Figure 1. (a) Beam-offset FDTR setup schematics. An actuator is used to steer an optical window to achieve offsets between pump and probe beams when needed. (b) Measurement and fit to the thermal phase obtained with 1.25 μm beam offset for the ML-3 structure (depicted in the inset).

In FDTR, samples are often coated with a thin metallic layer to act as both the heater and the thermometer. Although the presence of this transducer is often essential to improving the signal strength in FDTR measurements [31], its presence can reduce sensitivity to transport in the layers beneath, particularly if they have high thermal conductivity. In this work, we do not coat the samples with transducers as the Pt/Co multilayers have shown to possess a substantial thermoreflectance coefficient. The lack of the transducer leads to increased sensitivity to the heat transport in the multilayers.

The measured thermal phase spectrum is fitted to a diffusive heat equation solution where the unknown thermophysical properties can be extracted. It may be counterintuitive to use a diffusive model for data analysis in cases where non-diffusive transport could be taking place. However, non-diffusive transport would result in the apparent thermal parameters deviating from the expected values as well as the EDMM, and it can therefore be identified. The samples have been modeled by treating the multilayers along with the cap layer, the seed layer and Ta adhesive layer as a single effective medium as $ML/G_{ML/SiO2}/SiO_2(100)/G_{SiO2/Si}/Si$, where ML represents the thermal conductivity of the $Pt(2)/[Pt(t_{Pt})/Co(t_{Co})]_q/Pt(20)/Ta(1.5)$ layers. The model assumes all the heat is deposited on the surface of the multilayer. An alternative analysis that considers the finite light absorption depth is discussed in the Supplementary Information, but it does not affect the conclusions presented here.

The parameters of interest in this work are the out-of-plane (k_z) and in-plane (k_r) components of the anisotropic thermal conductivity of ML, as k_z will later be used to extract G for the Pt/Co interfaces. The sensitivity analysis of our measurement to the parameters of interest is provided in the Supplementary Information, along with the other known parameters used in the thermal model. Figure 1(b) shows an example for the thermal phase measured for sample ML-3 (t_{Pt} =

2.8nm, t_{Co} = 1.6nm, q = 32) and its corresponding fit. To estimate the uncertainties associated with the fitted thermal conductivity measured here, a Monte Carlo approach has been employed to determine the variations of the fitted k_r and k_z due to uncertainties in the most relevant thermal model parameters [31]. Accordingly, errors of ± 0.1 μm for the rms spot size and offset, and ± 1 MW/m^{2}K for $G_{SiO2/Si}$ have been considered over 300 iterations.

3. Results and Discussion

Figure 2(a) compares multilayer k_r extracted from FDTR fits with k_r extracted from the 4-point probe measurements by applying the Wiedemann-Franz law. Despite the difficulty of extracting k_r for the metallic layers via FDTR, due to the limited sensitivity of the experiment to in-plane transport (see Supplementary Information), the comparison shows a reasonably similar trend. The uncertainty in determining k_r does not affect the analysis and interpretation of k_z. These measurements indicate that the multilayers have an anisotropy k_r/k_z increasing from ~1.2 to ~2 as the interface density increases from ~0.03/nm to ~2/nm. We note that FDTR measures the total thermal conductivity due to both electron and phonon transport, whereas the 4-point probe measures electron transport only. Therefore, the somewhat higher value extracted through FDTR can be attributed in part to the additional contribution of phonon transport. Overall k_r is reduced by about a factor of 2 in the range of interface densities studied here. This effect can be attributed to increased scattering due to finite layer size [32,33].

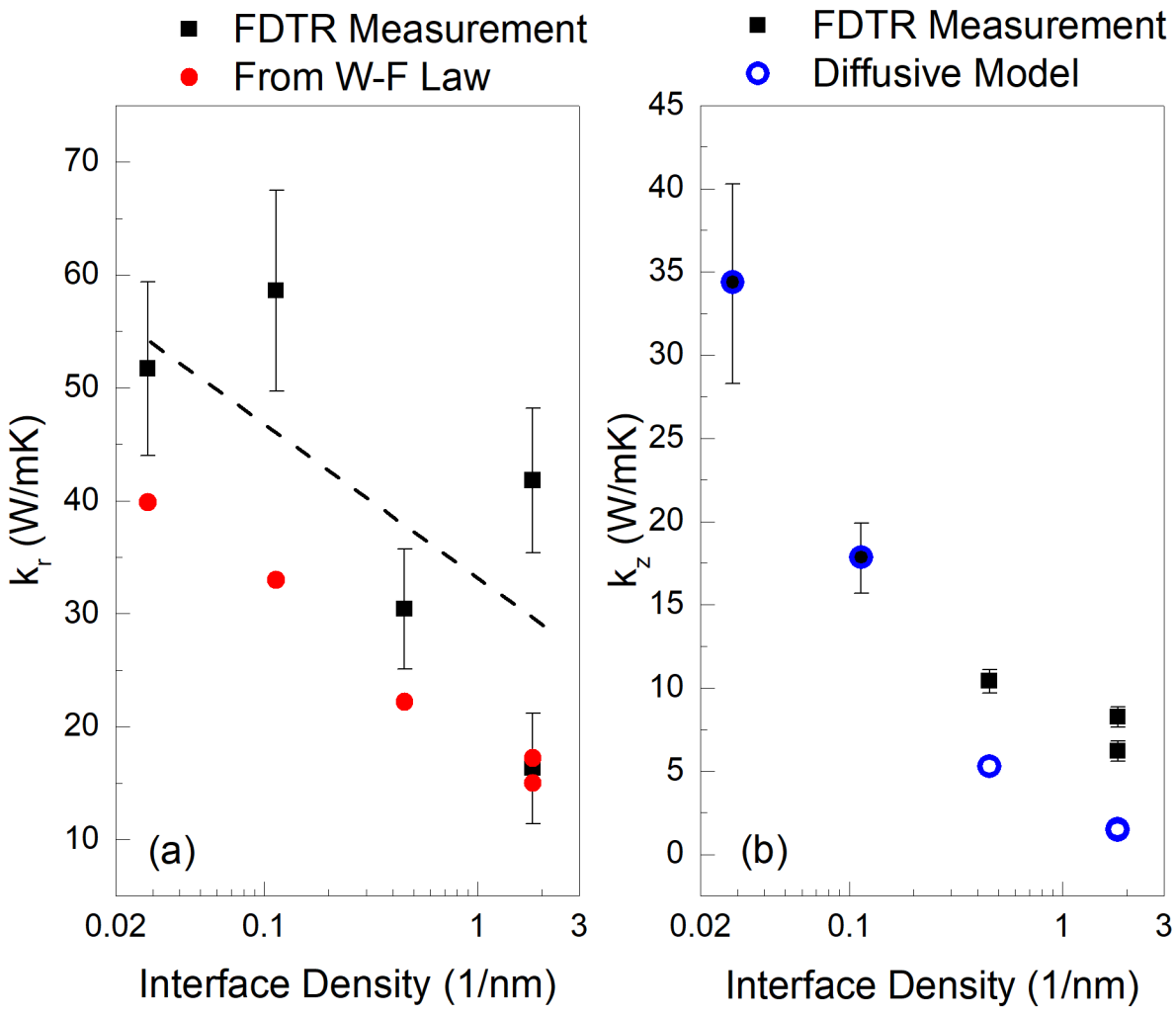

Figure 2. (a) Pt/Co multilayer in-plane thermal conductivity k_r as a function of interface density extracted from FDTR fits (squares) and 4-point probe through Wiedemann-Franz law (circles). The dashed line is a guide to the eye that shows the average offset between the FDTR and electrical data. (b) Pt/Co multilayer out-of-plane thermal conductivity k_z as a function of interface density from FDTR (square) and diffusive model (Eq. 1) with constant G of 2.5 GW/m^{2}K (circle). At the highest interface density point, two different samples have been measured, and for these the model prediction for k_z overlaps.

The effective out-of-plane thermal conductivity k_z is depicted in Figure 2(b) as a function of interface density. As expected, k_z decreases as the interface density increases due to the rising resistive contribution of the interfaces to the overall transport. For purely diffusive transport, the G of the Pt/Co interfaces could be related to k_z using [18]

$$\frac{t_{ML}}{k_z} = R_0 + \frac{n}{G_{Pt/Co}}, \qquad (1)$$

where t_{ML} is the thickness of the multilayer, R_0 is the total thermal resistance per Pt and Co layer unit area excluding the interfaces, and n is the number of interfaces. We set the value of R_0 as determined by the thermal conductivity for the in-plane direction; therefore, $R_0 = {t_{ML}}/{k_r}$. By extracting R_0 from the k_r values measured by FDTR in Figure 2(a) we can capture finite size and microstructural contributions to k_z. We make no assumptions for the Pt and Co layers' conductivity. The values for G obtained this way are depicted in Figure 3 as a function of interface density. The uncertainties in the values for G are determined by the error propagation Monte Carlo procedure outlined in the methods section, and the uncertainty is higher at low interface densities due to the small contribution the few interfaces have to the measured value of k_z. G is not constant beyond the experimental uncertainty and increases from a value of ~2.5 GW/m^{2}K at low interface densities to ~15 GW/m^{2}K at high interface densities – an indication of non-diffusive transport. This deviation from a diffusive model is also shown in Figure 2(b) where the result of Equation (1) is plotted for constant G = 2.5 GW/m^{2}K. Next, we will present how this data compares with theory and other literature data.

We start the theoretical analysis by estimating the maximum theoretical value of $G_{Pt/Co}$. The maximum transmission limit (MTL) for electrons, which is a special case of the EDMM, sets an upper limit for G in metallic interfaces by allowing perfect transmission, and is only limited by

the first and the second laws of thermodynamics [34]. Accordingly, the upper limit can be calculated by

$$G_{MTL} = \frac{v_f \gamma T}{4}, \qquad (2)$$

where v_f is the Fermi velocity, γ is the Sommerfeld parameter, and T is temperature with the product γT being the electronic volumetric heat capacity. Considering the (111) oriented *fcc* crystal structure confirmed by X-ray diffraction, we take the v_f value along this direction as $v_{f,Pt} = 2.37 \times 10^5\ ms^{-1}$ [35] and $v_{f,Co} = 3.3 \times 10^5\ ms^{-1}$ [36], and $\gamma_{Pt} = 400\ Jm^{-3}K^{-2}$ [20] and $\gamma_{Co} = 680\ Jm^{-3}K^{-2}$ [20] for the Sommerfeld parameters. We obtain $G_{MTL} = 7.11\ GW/m^2K$. Beyond this limiting case, according to the EDMM [17,18], the thermal boundary conductance is

$$G_{EDMM} = \frac{Z_1 Z_2}{4(Z_1+Z_2)}\ , \qquad (3)$$

where $Z = \gamma T v_f$. The subscripts refer to materials 1 and 2 on either side of the interface. Using the Fermi velocities and electronic heat capacities for Pt and Co, $G_{EDMM} = 5.0\ GW/m^2K$. The MTL and EDMM results are included in Figure 3.

For the samples with sub-nanometric layers (ML-1 and ML-2) having an interface density ~2/nm, a large deviation is observed from the predictions of MTL and EDMM. Since both MTL and EDMM are based on diffusive transport, we attribute this deviation to the non-diffusive nature of transport in these two samples because the mean free path of electrons is much larger than the period thickness in ML-1 and ML-2.

It is worth comparing $G_{Pt/Co}$ obtained in this work with that of Jang *et al*. [20], who measured it to be $> 8\ GW/m^2K$. Their experiment was performed on a Pt(42nm)/Co(0.8nm)/Pt(4nm)/sapphire sample consisting of two Pt/Co interfaces. The reason

they were able to set only a lower conductance bound was likely due to low measurement sensitivity to the two highly conductive interfaces.

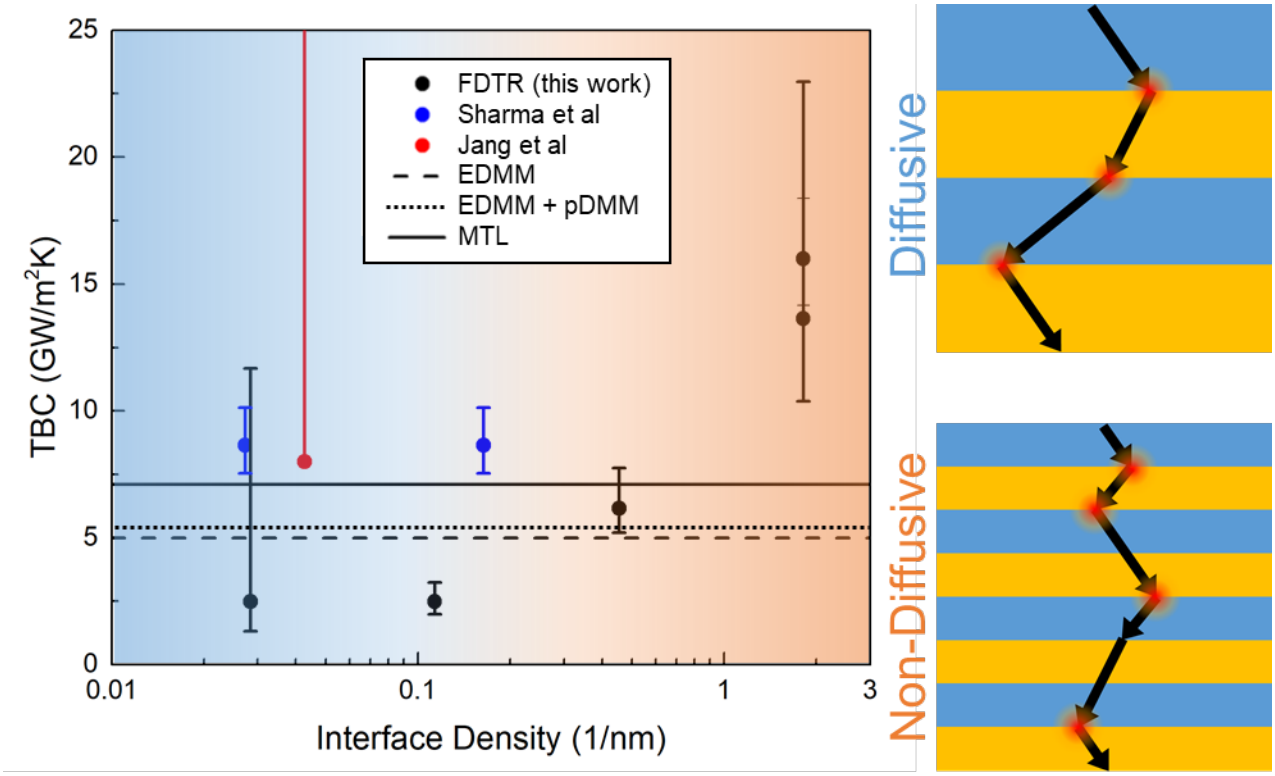

Figure 3. Pt/Co thermal boundary conductance extracted from FDTR fits compared with literature data from Sharma [38], Jang [20], and the predictions from EDMM, pDMM and MTL. The transport transitions from diffusive (G independent of interface density) to non-diffusive (G diverging) as the interface density increases. The schematics depict how electron transport might behave across interfaces in these regimes: for diffusive transport each interface can affect the electron energy distribution through inelastic scattering events, whereas for non-diffusive transport some scattering may be elastic or absent altogether. The result for non-diffusive transport is that conduction across the structure is higher than expected (Figure 2) and the average value of G per interface diverges.

Another method to infer metallic interface thermal conductance is through Current-Perpendicular-to-Plane (CPP) electrical resistivity measurements [37]. In CPP, the sample of interest is sandwiched between two contacts allowing a uniform current to pass through the sample. The interface specific resistance (*AR*, where *A* and *R* represent area through which current passes and sample resistance, respectively) is then extracted from the total sample specific resistance measured as a function of the number of interfaces for various samples [37]. Wilson and Cahill showed that the *AR* measurements of Pd/Ir layers can be related to *G* through the interfacial form of the Wiedemann-Franz law [18], expressed as

$$\frac{GAR}{T} = L_0, \qquad (4)$$

where L_0 is the Sommerfeld value of the Lorenz number ($2.45 \times 10^{-8}\ \Omega W K^{-2}$). Sharma *et al.* measured the Pt/Co interface specific resistance as $AR = 0.85 \pm 0.125\ f\Omega m^2$ [38], which translates to $G \sim 8.65 \pm 1.3\ GW/m^2K$ using the interfacial form of the Wiedemann-Franz law. We note that the literature data by Jang and Sharma are similar – close to G_{MTL} but obtained at interface densities below 0.2/nm.

So far in our discussion we have only considered electron transport under the assumption that it dominates transport in the metallic multilayers. Thermoreflectance measurements yield the total thermal conductivity, which consists of both electron and phonon carriers, so the FDTR data in Figure 3 reflects transport from both carriers. The Wilson and Cahill work indicates that the interfacial form of the Wiedemann-Franz law holds at room temperature for interface densities up to ~0.5/nm, and that the EDMM is sufficient to accurately describe the system [18]. The agreement between thermoreflectance measurements and EDMM in their work indicates that even at such relatively low k_z, thermal transport in the multilayer system is dominated by electrons.

In our measurements the higher value for k_r obtained by FDTR with respect to electrical conductivity measurements would point to a non-negligible phonon contribution to the total conductivity of the layers. This is also supported by the value we derived for $G_{Pt/Co}$, which is lower than the EDMM prediction, consistent with phonon contribution to the overall k_z being non-negligible. The onset of non-diffusive transport observed in Figure 3 appears for layer thickness well below the mean free path for both electrons and phonons. This opens the question of whether the non-diffusive transport we are observing originates from the electronic contribution, phononic contribution or both. While we cannot conclusively say which case applies here, there is indication that the electron transport dominates since the difference in FDTR and 4-point probe data points to electrons being the greatest contributor to the conductivity in Figure 2(a). We can include the phonon interface transport as a parallel conductance channel to the predicted total conductance $G_T = G_{EDMM} + G_{pDMM}$, where the phonon diffuse mismatch model (pDMM) can be calculated using known vibrational properties of Co and Pt [39]. The predicted value of G_{pDMM} = 400 MW/m^{2}K represents a contribution of less than 10% of the total interface conductance, and cannot account for the observations at high interface densities.

Future thermal conductivity measurements coupled with CPP electrical conductivity measurements at interface densities above 1/nm may further clarify the relative role of electrons and phonons and confirm whether the interfacial form of the Wiedemann-Franz law remains valid in this limit.

The increase in $G_{Pt/Co}$ has been interpreted here as evidence for non-diffusive transport, but the mechanism should be explored further. In the particle picture of transport, this would be an indication that carriers are not in equilibrium as they traverse the structure and quasi-ballistic

transport is present, but in the wave picture a diverging conductance is a sign of coherence [25]. The latter however seems unlikely for electron-mediated transport at room temperature, given the very small electron coherence lengths. While we do not observe a minimum in k_z for the interface density range explored in this work, one might speculate that k_z would increase in the limit where the Pt/Co layering is extended to monoatomic thickness as is the case for the thermal conductivity of L_10 ordered crystal phases as compared to equiatomic disordered alloys [40].

4. Conclusion

The anisotropic thermal conductivities of different Pt/Co multilayers were measured as a function of interface density. The Pt/Co interface thermal boundary conductance was extracted and compared with calculations from the electronic diffuse mismatch model. We showed an increase in boundary conductance at high interface densities, which might be arising from the non-diffusive heat transport at sub-nanometric scales. These results can inform how heat is dissipated in high interface density multilayers such as those found in magnetic memory and spintronic applications.

Acknowledgment

M.S., O.A. and S.P. acknowledge support by NSERC (Grant # RGPIN-2015-05221) and CFI (Grant # 35529). O.A. was also further supported by Mitacs (Grant # IT14782).

ASSOCIATED CONTENT

Supporting Information. The Supporting Information contains details of the FDTR sensitivity analysis, correlation analysis of the fitted parameters, and analysis of the effect of optical absorption depth on the extracted parameters.

REFERENCES

[1] Hohensee, G.T.; Biswas, M.M.; Pek, E.; Lee, C.; Zheng, M.; Wang, Y.; Dames, C. Pump-Probe Thermoreflectance Measurements of Critical Interfaces for Thermal Management of HAMR Heads. *MRS Advances* **2017**, *2* (58-59), 3627–3636.

[2] Huang, K.-F.; Wang, D.-S.; Lin, H.-H.; Lai, C.-H. Engineering spin-orbit torque in Co/Pt multilayers with perpendicular magnetic anisotropy. *Applied Physics Letters* **2015**, *107*, 232407.

[3] Choi, G.-M.; Moon, C.-H.; Min, B.-C.; Lee, K.-J.; Cahill, D.G. Thermal spin-transfer torque driven by the spin-dependent Seebeck effect in metallic spin-valves. *Nature Physics* **2015**, *11*, 576–581.

[4] Kimling, J.; Wilson, R.B.; Rott, K.; Kimling, J.; Reiss, G.; Cahill, D.G. Spin-Dependent Thermal Transport Perpendicular to the Planes of Co/Cu Multilayers. *Physical Review B* **2015**, *91* (14), 144405.

[5] Kimling, J.; Cahill, D.G. Spin diffusion induced by pulsed-laser heating and the role of spin heat accumulation. *Physical Review B* **2017**, *95* (1), 014402.

[6] Zhou, Q.; Huang, P.; Liu, M.; Wang, F.; Xu, K.; Lu, T. Grain and interface boundaries governed strengthening mechanisms in metallic multilayers. *Journal of Alloys and Compounds* **2017**, *698*, 906–912.

[7] Snel, J.; Monclús, M.A.; Castillo-Rodríguez, M; Mara, N.; Beyerlein, I.J.; Llorca, J.; Molina-Aldareguía, J.M. Deformation Mechanism Map of Cu/Nb Nanoscale Metallic Multilayers as a Function of Temperature and Layer Thickness. *The Journal of The Minerals* **2017**, *69*, 2214–2226.

[8] Zheng, S.; Beyerlein, I.J.; Carpenter, J.S.; Kang, K.; Wang, J.; Han, W.; Mara, N.A. High-strength and thermally stable bulk nanolayered composites due to twin-induced interfaces. *Nature Communications* **2013**, *4*, 1696.

[9] Jubert, P.; Santos, T.; L. E., T.; Ozdol, B.; Papusoi, C. Anisotropic Heatsinks for Heat Assisted Magnetic Recording. *IEEE Transactions on Magnetics* **2021**, *57* (2), 3200205.

[10] T.W. McDaniel, J. Phys. Condens. Matter 17, R315 (2005).

[11] Chiritescu, C.; Cahill, D. G.; Nguyen, N.; Johnson, D.; Bodapati, A.; Keblinski, P.; Zschack, P. Ultralow Thermal Conductivity in Disordered, Layered WS2 Crystals. *Science* **2007**, *315* (5810), 351.

[12] Goto, M.; Xu, Y.; T., Z.; Sasaki, M.; Nishimura, C.; Kinoshita, Y.; Ishikiriyama, M. Ultra-Low Thermal Conductivity of High-Interface Density Si/Ge Amorphous Multilayers. *Appl. Phys. Exp.* **2018**, *11*, 45202.

[13] Hua, Y.-C.; Cao, B.-Y. Interface-Based Two-Way Tuning of the in-Plane Thermal Transport in Nanofilms. *Journal of Applied Physics* **2021**, *123* (11), 114304.

[14] Li, Z.; Tan, S.; Bozorg-Grayeli, E.; Kodama, T.; Asheghi, M.; Delgado, G.; Panzer, M.; Pokrovsky, A.; Wack, D.; Goodson, K.E. Phonon Dominated Heat Conduction Normal to Mo/Si Multilayers with Period below 10 nm. *Nano Letters* **2012**, *12* (6), 3121–3126.

[15] Cahill, D.G. Analysis of Heat Flow in Layered Structures for Time-Domain Thermoreflectance. *Review of Scientific Instruments* **2004**, *75* (12), 5119–5122.

[16] Regner, K.T.; Majumdar, S.; Malen, J.A. Instrumentation of Broadband Frequency Domain Thermoreflectance for Measuring Thermal Conductivity Accumulation Functions. *Review of Scientific Instruments* **2013**, *84* (6), 64901.

[17] Gundrum, B.C.; Cahill, D.G.; Averback, R.S. Thermal Conductance of Metal-Metal Interfaces. *Physical Review B* **2005**, *72* (24), 245426.

[18] Wilson, R.B.; Cahill, D.G. Experimental Validation of the Interfacial Form of the Wiedemann-Franz Law. *Physical Review Letters* **2012**, *108* (25), 255901.

[19] Cheaito, R.; Hattar, K.; Gaskins, J.T.; Yadav, A.K.; Duda, J.C.; Beechem, T.E.; Ihlefeld, J.F.; Piekos, E.S.; Baldwin, J.K.; Misra, A.; Hopkins, P.E. Thermal Flux Limited Electron Kapitza Conductance in Copper-Niobium Multilayers. *Applied Physics Letters* **2015**, *106* (9), 93114.

[20] Jang, H.; Kimling, J.; Cahill, D.G. Nonequilibrium heat transport in Pt and Ru probed by an ultrathin Co thermometer *Physical Review B* **2020**, *101* (6), 064304.

[21] Choi, G.-M.; Wilson, R.; Cahill, D.G. Indirect heating of Pt by short-pulse laser irradiation of Au in a nanoscale Pt/Au bilayer. *Physical Review B* **2014**, *89* (6) 064307.

[22] Swartz, E.T.; Pohl, R.O. Thermal Boundary Resistance. *Review of Modern Physics* **1989**, *61* (3), 605–668.

[23] Gall, D. Electron mean free path in elemental metals. *Journal of Applied Physics* **2016**, *119* (8), 085101.

[24] Johnson, J.A.; Maznev, A.A.; Cuffe, J.; Eliason, J.K.; Minnich, A.J.; Kehoe, T.; Torres, C.M. S.; Chen, G.; Nelson, K.A. Direct Measurement of Room-Temperature Nondiffusive

Thermal Transport Over Micron Distances in a Silicon Membrane. *Physical Review Letters* **2013**, *110* (2), 025901.

[25] Simkin, M.V.; Mahan, G.D. Minimum Thermal Conductivity of Superlattices. *Physical Review Letters* **2000**, *84* (5), 927–930.

[26] Gurney, B.A.; Speriosu, V.S.; Nozieres, J.-P.; Lefakis, H.; Wilhoit, D.R.; Need, O.U. Direct measurement of spin-dependent conduction-electron mean free paths in ferromagnetic metals. *Physical Review Letters* **1993**, *71* (24), 4023–4026.

[27] Böhm, B.; Fallarino, L.; Pohl, D.; Rellinghaus, B.; Nielsch, K.; Kiselev, N.S.; Hellwig, O. Antiferromagnetic domain wall control via surface spin flop in fully tunable synthetic antiferromagnets with perpendicular magnetic anisotropy. *Physical Review B* **2019**, *100* (14), 140411.

[28] Hellwig, O.; Hauet, T.; Thomson, T.; Dobisz, E.; Risner-Jamtgaard, J.; Yaney, D.; Terris, B.; Fullerton, E.E. Coercivity tuning in Co/Pd multilayer based bit patterned media. *Applied Physics Letters* **2009**, *95* (23), 232505.

[29] Shahzadeh, M.; Rahman, M.; Hellwig, O.; Pisana, S. High-frequency measurements of thermophysical properties of thin films using a modified broad-band frequency domain thermoreflectance approach. *Review of Scientific Instruments* **2018**, *89* (8), 084905.

[30] Rahman, M.; Shahzadeh, M.; Braeuninger-Weimer, P.; Hofmann, S.; Hellwig, O.; Pisana, S. Measuring the thermal properties of anisotropic materials using beam-offset frequency domain thermoreflectance. *Journal of Applied Physics* **2018**, *123* (24), 245110.

[31] Rahman, M.; Shahzadeh, M.; Pisana, S. Simultaneous measurement of anisotropic thermal conductivity and thermal boundary conductance of 2-dimensional materials. *Journal of Applied Physics* **2019**, *126* (20) 205103.

[32] Mei S.; Knezevic, I. Thermal conductivity of III-V semiconductor superlattices. *Journal of Applied Physics* **2015**, *118* (17), 175101.

[33] Yang, B.; Chen, G. Partially coherent phonon heat conduction in superlattices. *Physical Review B* **2003**, *67* (19), 195311.

[34] Monachon, C.; Weber, L.; Dames, C. Thermal Boundary Conductance: A Materials Science Perspective. *Annual Review of Materials Research* **2016**, *46* (1), 433.

[35] Dye, D.H.; Ketterson, J.B.; Crabtree, G.W. The Fermi surface of platinum. *Journal of Low Temperature Physics* **1978**, *30*, 813–838.

[36] Petrovykh, D.Y.; Altmann, K.N.; Höchst, H.; Laubscher, M.; Maat, S.; Mankey, G.J.; Himpsel, F.J. Spin-dependent band structure, Fermi surface, and carrier lifetime of permalloy. *Applied Physics Letters* **1998**, *73*, 3459–3461.

[37] Acharyya, R.; Nguyen, H.Y.T.; Loloee, R.; Pratt Jr, W.P.; Bass, J.; Wang, S.; Xia, K. Specific resistance of Pd/Ir interfaces. *Applied Physics Letters* **2009**, *94* (2), 022112.

[38] Sharma, A.; Romero, J.; Theodoropoulou, N.; Loloee, R.; Pratt Jr, W.P.; Bass, J. Specific resistance and scattering asymmetry of Py/Pd, Fe/V, Fe/Nb, and Co/Pt interfaces. *Journal of Applied Physics* **2007**, *102* (11), 113916.

[39] Oommen, S. M; Pisana, S. Role of the electron–phonon coupling in tuning the thermal boundary conductance at metal-dielectric interfaces by inserting ultrathin metal interlayers. *Journal of Physics: Condensed Matter* **2021**, 33, 085702.

[40] Giri, A.; Wee, S.H.; Jain, S.; Hellwig, O.; Hopkins, P.E. Influence of chemical ordering on the thermal conductivity and electronic relaxation in FePt thin films in heat assisted magnetic recording applications. *Scientific Reports* **2016**, *6*, 32077.

TABLE OF CONTENTS GRAPHIC